

1 **Title: Regional and temporal variations affect the accuracy**
2 **of variant-specific SARS-CoV-2 PCR assays**

3

4 Running title: Designing PCR assays for SARS-CoV-2 variant detection

5

6 Chamteut Oh^{1,*}, Palash Sashittal^{2,*}, Aijia Zhou¹, Leyi Wang³, Mohammed El-Kebir², Thanh H.
7 Nguyen^{1,4}

8

9 **Equal contribution*

10 Corresponding authors: Thanh H. Nguyen (thn@illinois.edu) and Mohammed El-Kebir
11 (melkebir@illinois.edu)

12

13 1) Department of Civil and Environmental Engineering, University of Illinois at Urbana-
14 Champaign, United States

15 2) Department of Computer Science, University of Illinois at Urbana-Champaign, United States

16 3) Veterinary Diagnostic Laboratory and Department of Veterinary Clinical Medicine, University
17 of Illinois at Urbana-Champaign, United States

18 4) Institute of Genomic Biology, University of Illinois at Urbana-Champaign, United States

19

20

21 **Abstract**

22 Monitoring the prevalence of SARS-CoV-2 variants is necessary to make informed public health
23 decisions during the COVID-19 pandemic. PCR assays have received global attention, facilitating
24 rapid understanding of variant dynamics because they are more accessible and scalable than
25 genome sequencing. However, as PCR assays target only a few mutations, their accuracy could be
26 compromised when these mutations are not exclusive to target variants. Here we show how to
27 design variant-specific PCR assays with high sensitivity and specificity across different
28 geographical regions by incorporating sequences deposited in the GISAID database. Furthermore,
29 we demonstrate that several previously developed PCR assays have decreased accuracy outside
30 their study areas. We introduce PRIMES, an algorithm that enables the design of reliable PCR
31 assays, as demonstrated in our experiments to track dominant SARS-CoV-2 variants in local
32 sewage samples. Our findings will contribute to improving PCR assays for SARS-CoV-2 variant
33 surveillance.

34

35 **Key words:** PCR assays; SARS-CoV-2 variants; *in silico* analysis; PRIMES; Wastewater-based
36 epidemiology.

37

38

39 **Importance**

40 Monitoring the introduction and prevalence of variants of concern (VOCs) and variants of interest
41 (VOIs) in a community can help the local authorities make informed public health decisions. PCR
42 assays can be designed to keep track of SARS-CoV-2 variants by measuring unique mutation
43 markers that are exclusive to the target variants. However, the mutation markers can not be
44 exclusive to the target variants depending on regional and temporal differences in variant dynamics.
45 We introduce PRIMES, an algorithm that enables the design of reliable PCR assays for variant
46 detection. Because PCR is more accessible, scalable, and robust to sewage samples over
47 sequencing technology, our findings will contribute to improving global SARS-CoV-2 variant
48 surveillance.

49

50

51

52

53 **Introduction**

54 SARS-CoV-2 has had an unprecedented impact on public health globally. However, despite the
55 availability of vaccines, emerging new variants, which may have better infectivity, transmissibility,
56 and immune evasion, threaten global public health again (1, 2). Monitoring the introduction and
57 prevalence of variants of concern (VOCs) and variants of interest (VOIs) in a community can help
58 the local authorities make informed decisions regarding public health (3–5). In particular,
59 wastewater-based epidemiology (WBE) has been applied across the globe to monitor SARS-CoV-
60 2 circulating in a community (6–9). WBE could complement clinical diagnosis because WBE
61 allows health authorities to monitor transmission levels in communities, including asymptomatic
62 patients, without requiring excessive resources (10).

63 Although sequencing is considered the gold standard to identify SARS-CoV-2 lineages,
64 PCR assays have attracted global attention for variant detection due to several advantages (11).
65 First, PCR is a more accessible tool because the instruments and reagents are more affordable.
66 Second, PCR is more scalable because it can analyze dozens or hundreds of samples in only a few
67 hours, while sequencing takes a much longer time (>12 hours) (12). Third, PCR is more robust to
68 sewage samples that have low concentrations of SARS-CoV-2 genomes and contain different
69 types of impurities (13). These advantages are beneficial to ramp up capacity for SARS-CoV-2
70 surveillance and facilitate deployment in regions where there is a lack of access to sequencing
71 facilities to initiate their variant monitoring systems.

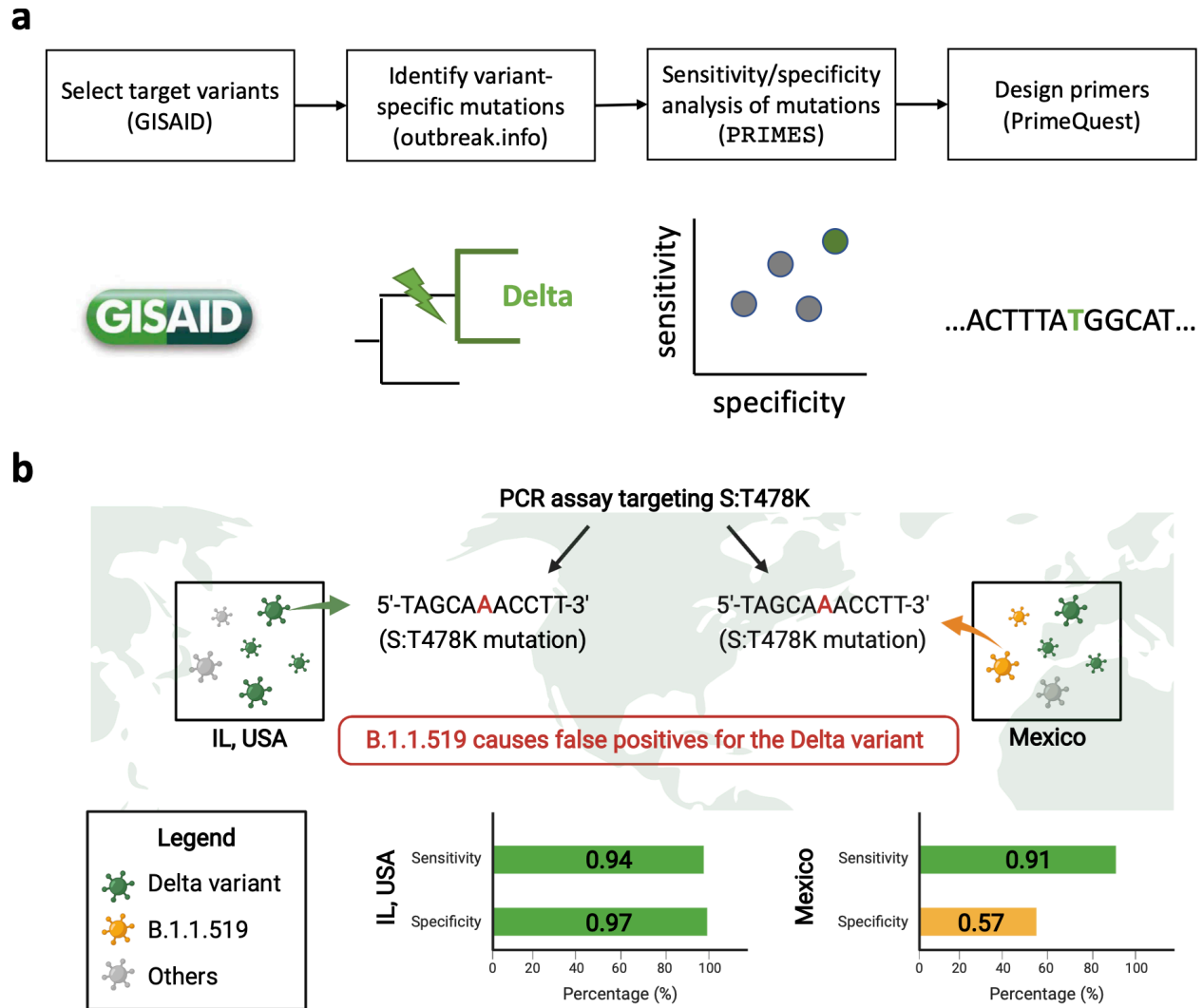
72 PCR assays are composed of about 20 to 30 base pair long primers or probes designed to
73 detect single or multiple loci that characterize a target variant. Importantly, PCR assays can only
74 examine less than 100 bp long sequences, while sequencing produces reads that span longer
75 genome regions (> 1000 bp). Meanwhile, each variant or sub-lineage of SARS-CoV-2 is defined

76 by a group of different mutations located throughout the entire genome. Therefore, distinct variants
77 may have the same mutations, reducing specificity when used in PCR assays (14).

78 In this study, we introduce a computational tool, PRIMES (PRIMER Efficacy Sleuth), that
79 can be used to analyze sequences available in open source databases such as GISAID (15, 16), to
80 predict the sensitivity and specificity of a PCR assay to detect specific pathogen lineages of interest
81 (**Fig. 1a**). Moreover, for a given set of mutations characterizing the target variant, PRIMES can
82 also identify a subset of variant-specific mutations for designing PCR assays with high specificity
83 and sensitivity. Using PRIMES, we show multiple examples of previous PCR assays (13, 17, 18)
84 that were successfully applied to certain study areas that might not work for other regions (**Fig.**
85 **1b**). We also demonstrate that the PCR assays designed using PRIMES successfully identify the
86 dominant lineages in sewage samples from Champaign County, IL, USA. We conclude that PCR
87 assays ought to be designed or modified considering regional and temporal variations and that *in*
88 *silico* analyses using open source databases can address the weaknesses of PCR assays. These
89 findings will allow PCR assays to be applied more reliably for SARS-CoV-2 surveillance.

90

91



92

93 **Fig. 1.** (a) A schematic describing the workflow for designing PCR assays while considering
 94 regional and temporal variations in GISAID samples. After selecting a target variant, we identify
 95 variant-specific mutations, which we rank in terms of sensitivity and specificity using the
 96 introduced tool PRIMES. Finally, we design primers for mutations with high sensitivity and
 97 specificity for the geographical region of interest. (b) An illustration showing the effect of regional
 98 lineages on the accuracy of variant-specific PCR assays.

99

100 **Results**

101 **Analysis and design of PCR assays using PRIMES**

102 As new variants of SARS-CoV-2 emerge and fade away throughout the world, a number
103 of different lineages (1340 lineages as of August 2021) have been reported (19). Due to the
104 evolutionary relationship of these lineages, they often share characteristic mutations. As such, PCR
105 assays targeting only a few mutations (typically 1-3 mutations) have difficulty detecting samples
106 from a specific lineage of interest with high specificity and sensitivity. In addition, while most
107 lineages are limited to where they emerged, outbreaks of some lineages occasionally spread across
108 the borders and become global concerns (such as variants of concern (VOCs) and variants of
109 interest (VOIs)). Thus, regional and temporal differences in variant dynamics have to be
110 considered for PCR assays.

111 The most widely used computational tool for assigning lineages to SARS-CoV-2 genomes
112 is the Phylogenetic Assignment of Named Global Outbreak Lineages (Pangolin,
113 <https://pangolin.cog-uk.io/>). Pangolin is a lineage designation pipeline that takes a FASTA file as
114 input, containing one or more query sequences. Each query sequence is first aligned to the SARS-
115 CoV-2 reference genome (Wuhan-Hu-1, NC_045512.2) using minimap2 v2.17 (20). After
116 trimming the non-coding regions in the 5' and 3' ends of the aligned sequences, they are assigned
117 to the most likely lineage out of all [currently designated lineages](#) using an underlying machine
118 learning model referred to as PangoLEARN. The current version of PangoLEARN is a decision
119 tree that is trained on data from GISAID that was manually curated with lineages.

120 By considering the lineage designation of Pangolin as ground truth, we perform an *in silico*
121 analysis of the efficacy of PCR assays using PRIMES (available at [https://github.com/elkebir-](https://github.com/elkebir-group/primes)
122 [group/primes](https://github.com/elkebir-group/primes)). Specifically, we search for the target sequence (containing a mutation targeted by

123 the PCR assay) in each GISAID sequence and then estimate the overall specificity and sensitivity
124 of the PCR assay. While this information is crucial in its own right, it can also be used to design
125 lineage-specific PCR assays. Specifically, for a lineage of interest and a set of characteristic
126 mutations, we use PRIMES to identify the set of mutations that should be targeted by PCR assays
127 to get high specificity and sensitivity. We employ this approach to design PCR assays to detect the
128 presence SARS-CoV-2 of both Alpha (e.g., B.1.1.7) and Delta (e.g., B.1.617.2) variants in sewage
129 samples.

130

131 **Analysis of previously developed PCR assays**

132 Here, we use PRIMES to analyze the efficacy of previously developed PCR assays targeting
133 specific Spike (S) protein mutations in the SARS-CoV-2 genome. Recall that sensitivity and
134 specificity are defined as follows.

135

$$136 \text{ Sensitivity} = \frac{\textit{True positive}}{\textit{True positive} + \textit{False negative}} \quad (\text{Eq. 1})$$

$$137 \text{ Specificity} = \frac{\textit{True negative}}{\textit{True negative} + \textit{False positive}} \quad (\text{Eq. 2})$$

138

139 where true positive indicates the number of virus sequences that include the primer sequences and
140 also belong to the lineage of interest. False negative is the number of virus sequences that do not
141 include the primer sequences but belong to the lineage of interest. True negative is the number of
142 virus sequences that do not include the primer sequences and do not belong to the lineage of
143 interest as well. Finally, false positive indicates the number of virus sequences that include the
144 primer sequences but belong to the lineage of interest. Strikingly, our analysis shows that several

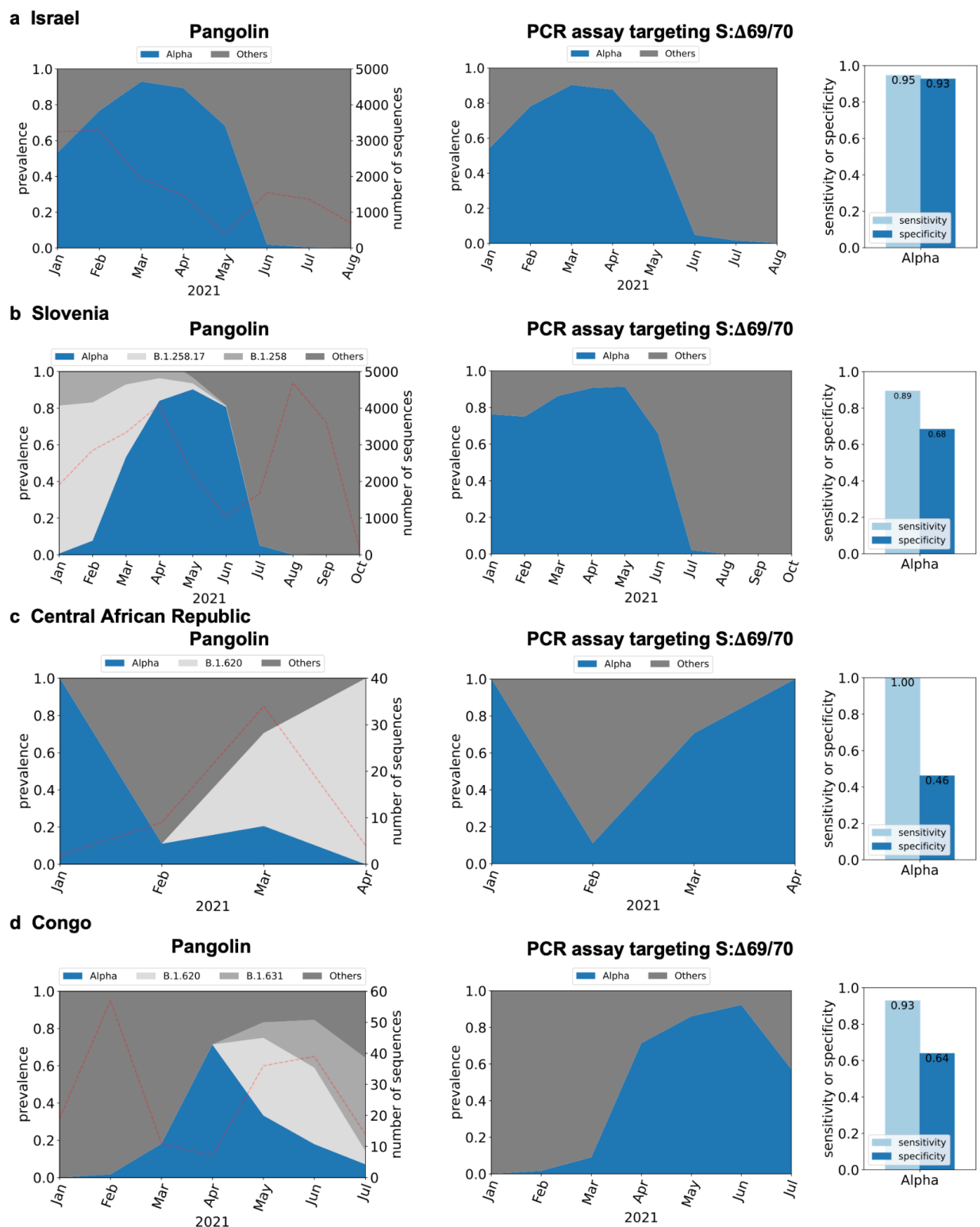
145 previously developed PCR assays would not be as accurate for samples collected from locations
146 and periods beyond those included in the original study.

147 First, we focus on analyzing PCR assays targeting S:Δ69/70 to detect the Alpha variant (13,
148 17, 21). These PCR assays were verified with synthetic RNA controls and local sewage samples
149 from Israel. Then, we simulated the application of these assays to sequences deposited in GISAID
150 for Israel (n=13932 from January 2021 to October 2021). **Fig. 2a** shows that the Alpha variant was
151 dominant (most prevalent variant) from January 2021 until May 2021, after which most samples
152 were from other lineages. PRIMES predicts that the PCR assays targeting S:Δ69/70 (17) correctly
153 assigned GISAID samples to the Alpha variants with a sensitivity of 0.95 and a specificity of 0.93.
154 This finding can be attributed to the observation that the target mutations of these PCR assays,
155 S:Δ69/70, is mostly exclusive to the Alpha variant in Israel, where this PCR assay was developed.
156 However, although S:Δ69/70 was once a key mutation for the Alpha variant (B.1.1.7 first reported
157 in February 2020), B.1.258.17 (first reported in August 2020) and B.1.620 (first reported in
158 February 2021) and more lineages are also known to have the same mutation. Although these
159 SARS-CoV-2 lineages are not significant in Israel (29/13932), they have significant prevalence in
160 certain regions at some points in time due to local outbreaks. For example, the B.1.258.17 lineage
161 accounted for 21.8% of all the sequences on GISAID from Slovenia for the period between January
162 2021 to October 2021.

163 While this PCR assay targeting S:Δ69/70 was only applied to wastewater samples from
164 Israel in the previous study (17), we can use PRIMES to predict the sensitivity and specificity of
165 this PCR assay on GISAID samples from any other region. **Fig. 2b** shows our analysis on samples
166 from Slovenia (n=25528, from January 2021 to October 2021) where the prevalence of lineage
167 B.1.258.17 was significant until May 2021 and dominating in January 2021 and February 2021.

168 On the other hand, Alpha variant has less than 10% prevalence in January 2021 and February 2021.
169 However, our analysis of the PCR assays shows that the Alpha would have been dominant from
170 January 2021 until June 2021. This error came from the fact that these assays would have
171 incorrectly assigned genomes belonging to the B.1.258 and B.1.258.17 lineages to the Alpha
172 variant. The false positives for the Alpha variant continued until June 2021 the B.1.258.17 lineage
173 fades out. Thus, while the estimated sensitivity of the assay for the Alpha variant in Slovenia is
174 0.89, the specificity is estimated to be only 0.68. We also found that PCR assays targeting S:Δ69/70
175 could lead to significant amounts of false positives when applied to samples from the Central
176 African Republic (**Fig. 2c** shows that the estimated specificity is only 0.46 due to samples from
177 B.1.620), Republic of Congo (**Fig. 2d** shows that the estimated specificity is only 0.64 due to
178 B.1.620 and B.1.631).

179



180

181 **Fig. 2.** *In silico* analysis of PCR assay targeting S:Δ69/70 mutation (17) to detect the Alpha variant
 182 for GISAID samples from (a) Israel (n=13,932), (b) Slovenia (n=25,528), (c) Central African
 183 Republic (n=49) and (d) Congo (n=183). Dotted lines on left figures indicate the number of
 184 sequences used for the *in silico* analyses.

185

186 We conducted a similar analysis for another PCR assay targeting mutation S:Δ144/145 to
187 detect the Alpha variant (13). This assay was applied to samples from wastewater treatment plants
188 and selected residential buildings across the USA to track the occurrence of the Alpha variant over
189 time in 19 communities. **SI Fig. 1a** shows that this assay works well for GISAID sequences from
190 the USA with estimated sensitivity and specificity of 0.90 and 0.98, respectively. However, several
191 lineages including C.1.2, B.1.620, B.1.1.318, B.1.525 (or the Eta variant), B.1.637, B.1.625, and
192 AZ.2 also have the same mutation S:Δ144/145 targeted by this assay. This PCR assay can produce
193 false results if any of the aforementioned lineages have significant prevalence in the area being
194 studied. For example, we analyzed GISAID sequences collected from Gabon (n=254, from January
195 2021 to May 2021). **SI Fig. 1b** suggests that Gabon had significant sequences from the Eta variant
196 and the B.1.1.318 lineage from February 2021 to May 2021, both of which have the target mutation
197 S:Δ144/145 mutation. As a result, even though the number of sequences from the Alpha variant
198 increased from February 2021 to April 2021 and then decreased in May 2021, the PCR assay
199 would have predicted a continuous increase in the prevalence of the Alpha variant from February
200 2021 to May 2021 (**SI Fig. 1b**). The estimated specificity of this assay for detecting the Alpha
201 variant on GISAID sequences from Gabon is only 0.74. We see a similar result by analyzing
202 GISAID sequences from Togo (n=157 from January 2021 to April 2021) in **SI Fig. 1c**. In fact,
203 many countries in Africa, including Nigeria and Ghana, were also expected to have lower
204 specificity for the PCR assay targeting S:Δ144/145 because of B.1.1.338 and B.1.525 lineages (**SI**
205 **Table 1**).

206

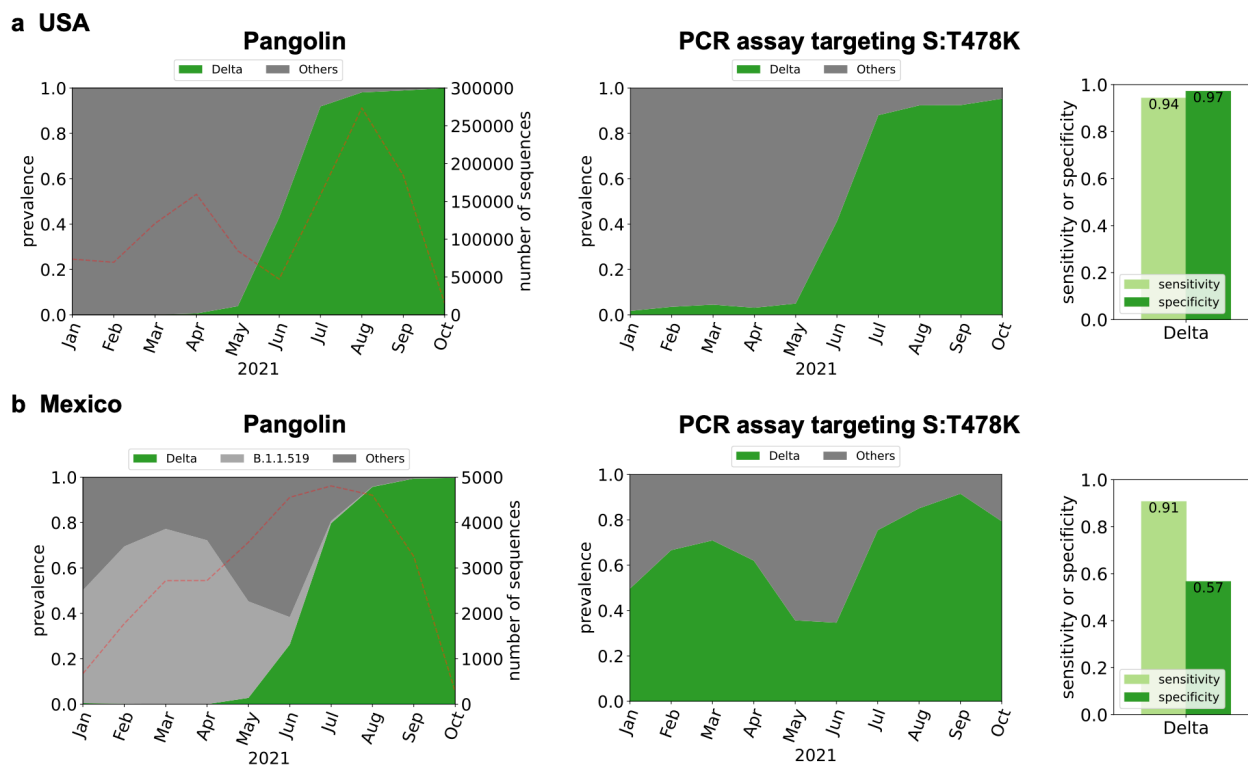
207

208 This propensity for false positive results is not limited to PCR assays developed to detect
209 samples from the Alpha variant. We demonstrate this by considering a recent PCR assay targeting
210 mutation S:T478K of the Delta and Delta plus lineages (18). However, this mutation is also present
211 in the B.1.1.519 lineage. This lineage accounted for only around 1.2% of sequences from the USA
212 (n=1,187,412 from January 2021 to October 2021), so the PCR assay targeting S:T478K was
213 expected to work well for IL, USA, showing 0.94 of estimated sensitivity and 0.97 of estimated
214 specificity (**Fig. 3a**). However, the B.1.1.519 lineage was dominant in Mexico (n=28,956) and
215 explained 30% of the total GISAID sequences from January 2021 to October 2021 (**Fig. 3b**).
216 Therefore, our analysis shows that the PCR assay targeting S:T478K would estimate that the Delta
217 variant was dominant all the way from January 2021 to October 2021, when in reality, Delta variant
218 sequences were collected and later deposited in GISAID, starting May 2021 (**Fig. 3b**).

219

220

221



222

223 **Fig. 3.** *In silico* analysis of PCR assay targeting S:T478K mutation (18) to detect the Delta variant:
 224 (a) USA (n=1,187,412) and (b) Mexico (n=28,956). Dotted lines on left figures indicate the
 225 number of sequences used for the *in silico* analyses.
 226

227 The examples of regional and temporal characteristics affecting the accuracy of PCR
 228 assays for the detection of SARS-CoV-2 samples of specific lineages of interest are not limited to
 229 the cases mentioned above. Globally, only a few VOCs and VOIs accounted for higher than 1%
 230 of the total sequences in GISAID, while most of other SARS-CoV-2 lineages explain less than 1%.
 231 However, as we examine narrower regions, we may find outbreaks of certain lineages that could
 232 be overlooked when we focus on the prevalence on a global scale. For example, as of October
 233 2021, B.1.526 lineage accounted for 1% of reported sequences in the world. However, the
 234 prevalence of the lineage increases as we narrow down the study area to local: 4% in the U.S., 17%
 235 in New York state, and 30% in Bronx country. In the case of B.1.429 lineage, the prevalences are
 236 1%, 4%, 11%, and 38% in the world, the U.S., California State, and Riverside County, respectively.

237 The number of B.1.258 lineage was less than 0.5% of total sequences worldwide, but it accounted
238 for 54% of cases in Cyprus.

239 We summarized SARS-CoV-2 lineages that have the same mutation that our target variant
240 possesses in **SI Table 1**. When we use PCR assays targeting certain mutations, this table will help
241 identify the lineages that would interfere with our PCR assay. In **SI Table 2**, we also tabulated
242 countries where each of the SARS-CoV-2 lineages summarized in **SI Table 1** accounted for higher
243 than 1% of total sequences. This table will explain whether the lineages that would interfere with
244 your PCR assays are dominant in the study areas. By interpreting **SI Table 1** and **SI Table 2**
245 together, we can find various examples where certain PCR assays would not work reliably. In
246 conclusion, the findings that previously developed PCR assays would not work for certain regions
247 due to the presence of lineages sharing some unique mutations with other lineages motivated us to
248 establish PCR assays for variant detection based on the characteristics of sequences reported from
249 our target study area (IL, USA).

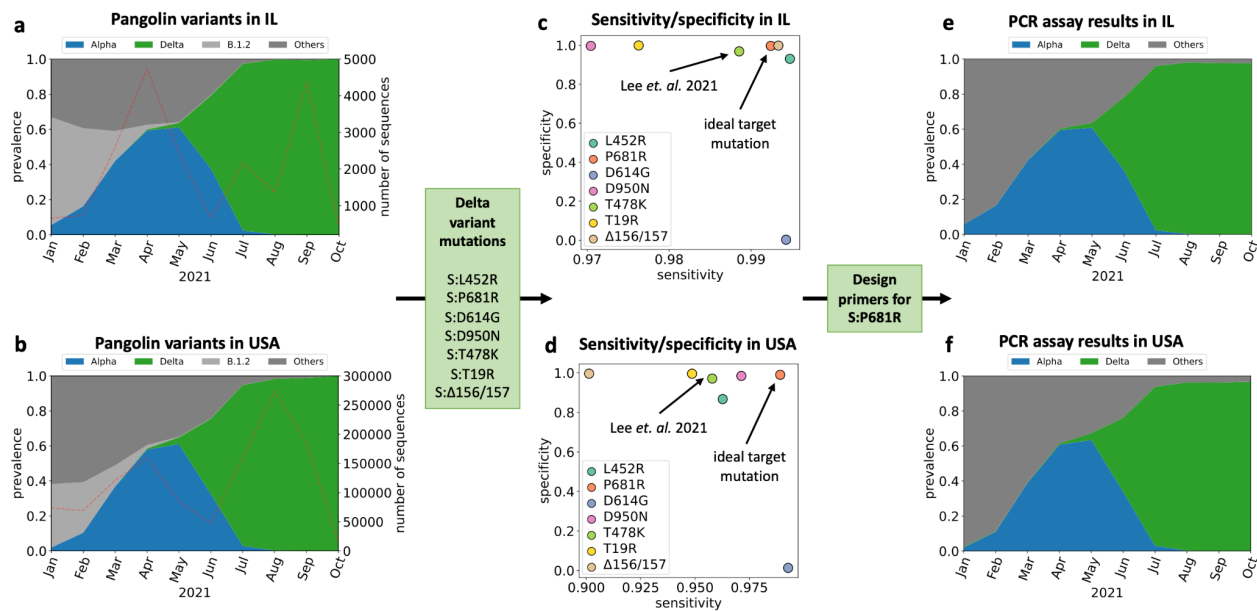
250

251 **Design of variant-specific PCR assays considering regional and temporal characteristics**

252 We describe the proposed workflow to design variant-specific PCR assays considering regional
253 and temporal variant dynamics using PRIMES (**Fig. 1a**). Our goal is to design variant-specific
254 PCR assays to track variants with significant prevalence in the USA, with a particular focus on the
255 state of Illinois.

256 First, we investigated the prevalence of SARS-CoV-2 lineages in our regions of interest to
257 select lineages that we need to track. To this end, we downloaded 1,187,412 SARS-CoV-2
258 sequences from GISAID collected between January 2021 and October 2021 in the USA, including
259 20,165 sequences collected in Illinois. These sequences were assigned to the most likely lineage

260 using Pangolin (**Fig. 4a, b**). Focusing on the variant dynamics in the state of Illinois (**Fig. 4a**), we
261 observe that the B.1.2 lineage was dominant from January (61%) to February (44%), eventually
262 giving way to the Alpha variant. The Alpha variant became dominant in April (44%), May (61%),
263 and June (62%). Then, the Delta variant samples replaced the Alpha variant samples and has been
264 the dominant lineage in the state (95% in July and >99% in August, September and October).
265 Other VOIs and VOCs, including Epsilon, Iota, and Beta variants, accounted only for 2.2%, 1.5%,
266 and 0.4% of total sequences, respectively. Similar trends were observed in sequences collected
267 throughout the USA (**Fig. 4b**). Based on the variant dynamics of our regions of interest, we decided
268 to design PCR assays to enable monitoring of the two major variants, the Alpha and the Delta
269 variants.
270



271

272 **Fig. 4.** Variant dynamics determined by Pangolin using GISAID samples from (a) the state of
 273 Illinois in USA (n=20,165) and (b) USA (n=1,187,412). Focusing on the spike protein mutations
 274 in the Delta variant, we show the sensitivity and specificity of assigning the Delta variant based
 275 on the presence of each mutation in GISAID samples from (c) IL and (d) USA. The estimated
 276 assignment of GISAID samples from (e) IL and (f) USA to variants using the primer designed to
 277 target mutation S:P618R.

278

279 Second, we designed PCR assays to find unique mutations that are exclusive to our lineage
 280 of interest. We utilized <https://covariants.org> to list up nonsynonymous mutations that define target
 281 variants (SI Table 1). We focused on mutations located in the spike gene, which has a higher
 282 frequency of mutation than other SARS-CoV-2 genes (22). Previous studies have shown that
 283 primers targeting mutations in the spike gene enable accurate detection of SARS-CoV-2 lineages
 284 in sewage samples with low virus concentration (21). As a result, for the Alpha variant, we identify
 285 9 mutations in the spike gene – S:Δ69/70, S:Δ144, S:N510Y, S:A570D, S:D614G, S:P681H,
 286 S:T716I, S:S982A, and S:D1118H. For the Delta variant we identify 7 mutations – S:T19R,
 287 S:Δ156/157, S:L452R, S:T484K, S:D614G, S:P681R, and S:D950N. Note that mutation S:T484K
 288 was targeted by the PCR assay to detect the Delta and Delta plus variant (18).

289 Third, we used PRIMES to compute the sensitivity and specificity of lineage assignments
290 performed using each of the selected mutations. We assumed if the specificity and sensitivity of
291 the mutations are higher than 0.99, the mutations are exclusive to the target variant. This criterion
292 allows us to identify the ideal target mutation for the design of the PCR assay that would yield
293 high specificity and sensitivity in our regions of interest. For the Alpha variant, we found three
294 acceptable mutations (S:A570D, S:T716I, and S:S982A) (**SI Fig. 2b**), and we chose the S:A570D
295 mutation because PCR assay targeting S:A570D has already been verified to work for sewage
296 samples, we adopted this mutation in our analysis (13). For the Delta variant, we found three
297 acceptable mutations (S:L452R, S:P681R, and S:Δ156/157) with GISAID samples from the state
298 of Illinois. However, if we look at all GISAID samples from the USA, the sensitivity for S:L452R
299 and S:Δ156/157 mutations to characterize the Delta variant drops below 0.97. Thus, regional
300 variation can lead to a drastic change in the performance of variant-specific PCR assays. Since our
301 goal is to develop PCR assays that are effective in other states besides Illinois in the USA as well,
302 we instead choose S:P681R, which has high sensitivity and specificity in both Illinois (sensitivity
303 is 0.99 and specificity is 0.99) as well as the USA (sensitivity is 0.99 and specificity is 0.99).
304 Importantly, this mutation has higher sensitivity and specificity in both regions of interest
305 compared to mutation S:T478K (sensitivity is 0.99 and specificity is 0.97 in Illinois, while
306 sensitivity is only 0.96 and specificity is only 0.98 in the USA, see **Fig. 4c,d**) that previously
307 targeted to monitor the Delta and Delta plus variants (18).

308 The fourth step is to design the allele-specific primers for the selected mutations. Since
309 both our selected target mutations are single nucleotide polymorphisms (SNPs), we designed
310 allele-specific qPCR assays in which either a forward or a reverse primer target the SNP at the 3'
311 end with a mismatch near the SNP location to improve the specificity of the assays (13). All RT-

312 qPCR assays were designed using PrimerQuest (Integrated DNA Technologies; IDT, USA) to
313 have an annealing temperature from 58 to 63 °C for primers and GC contents from 30 to 60%.

314 Finally, we can estimate the efficacy of the candidate RT-qPCR assays using PRIMES.
315 Specifically, we determine the sensitivity and specificity of our assays on the GISAID samples
316 collected from the regions of interest by searching for sequences of a forward primer and a reverse
317 primer in each query sequence. Note that the sequences of reverse primers were converted to
318 reverse sequences to have all sequences, including primers and viruses, on the same strand. If the
319 viral sequence includes the forward and reverse sequences, we assumed that the PCR assay would
320 detect the viral sequence (an illustrative example is shown in **SI Fig. 3**). We note that operational
321 failures of the assay due to inappropriate primer design or PCR inhibitors are not considered by
322 PRIMES. Some lineages should be expected to lower the sensitivity or specificity of our assays
323 based on **SI Table 1** (e.g., B.1.1.189, C38, and B.1.636 for the Alpha variant detection and AU.3,
324 AU.2, P.1.8, B.1.617.3, A.23.1, B.1.617.1, B.1.551, B.1.466.2, B.1.1.528, Q.4, B.1.623, B.1.1.25,
325 C.36, and AY.28 for the Delta variant detection), but importantly those lineages were not detected
326 or had very low prevalence in our regions of interest. The estimated sensitivity and specificity for
327 PCR assays designed to detect viruses from the Alpha and Delta variants were all high for our
328 study scope, and in Illinois in particular (sensitivity is 0.99 and specificity is 0.99 for detection of
329 Alpha variant and sensitivity is 0.98 and specificity is 1.00 for detection of the Delta variant in
330 Illinois, see **SI Fig. 4**, for sensitivity and specificity of detecting the two variants in GISAID
331 samples from all of the USA). These values are higher than the sensitivity and specificity estimated
332 for the previously developed PCR assays in their regions of interest (see **Fig. 2** and **3**). In the
333 subsequent section, we demonstrate this performance of our PCR assays translated to synthetic
334 controls and actual sewage samples collected in our community.

335

336 **Verification of PRIMES-designed PCR assays by synthetic RNA controls**

337 We applied the RT-qPCR assays designed with PRIMES to synthetic RNA controls for
338 WT, Alpha, and Delta variants to experimentally confirm the sensitivity (i.e., the limit of
339 quantification; LOQ and limit of detection; LOD) and specificity (i.e., cross-reactivity). Regarding
340 sensitivity, we found that the LOQs for total SARS-CoV-2, Alpha variant, and Delta variant were
341 all 10 gene copies (gc)/ μL or 50, 30, and 30 gc/reaction, respectively (**SI Fig. 5a**). Also, the LODs
342 of RT-qPCR assays for total SARS-CoV-2, Alpha variant, and Delta variant were 1.0, 1.3, and 1.3
343 gc/ μL or 5.0, 3.9, and 3.8 gc/reaction, respectively (**SI Fig. 5b**). Because LODs for our assays
344 were close to the theoretical LODs of RT-qPCR (3.0 gc/reaction)(23), we concluded that our RT-
345 qPCR assays are sensitive to detect RNA of target variants.

346 As for the cross-reactivity, we found that when the concentrations of the RNA synthetic
347 control were high (i.e., 10^4 and 10^5 gc/ μL), we detected Cq values from WT RNA controls. This
348 finding suggests that the presence of WT caused false positives for the Alpha variant detection
349 (**SI Fig. 6a**). However, the Cq value differences between the Alpha variant and WT were greater
350 than 11 that is about 10^3 -fold difference in RNA concentrations. This difference in Cq values is
351 equivalent to less than 0.1% error when quantifying the Alpha variant, and thus we considered this
352 error is acceptable for our study. When the RNA synthetic control concentrations were low (i.e.,
353 less than 10^3 gc/ μL), the Cq values from WT were lower than LOD, which will be disregarded in
354 this study, so the false positives were not detected. We found similar results from the specificity
355 experiments for the Delta variant assay (**SI Fig. 6b**). When the concentrations of the RNA synthetic
356 controls were high (i.e., 10^4 and 10^5 gc/ μL), the Cq value differences from Delta variant and WT
357 were greater than 13. At the lower concentration (i.e., less than 10^3 gc/ μL), the Cq values from

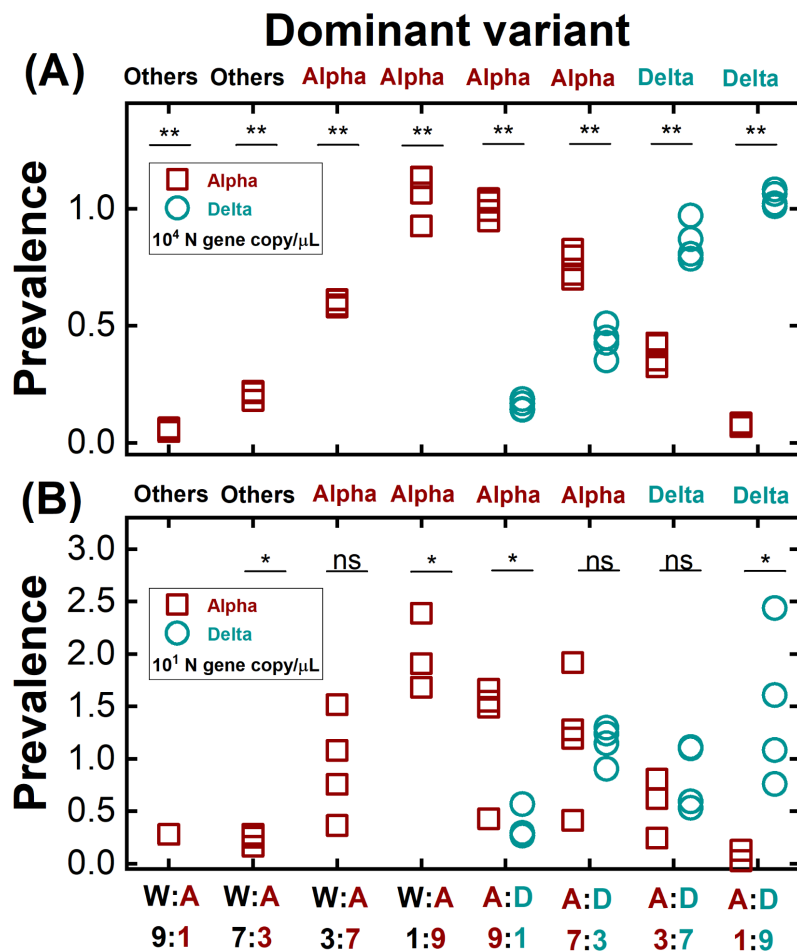
358 WT (i.e., false positives) were less than LOD. Because the measured cross-reactivities by WT were
359 negligible, we concluded our RT-qPCR assays are specific to measure target variants.

360 We further confirmed the applicability of PRIMES-designed PCR assay to determine
361 predominant variants in mixtures of synthetic RNA controls. The results from the mixtures of
362 synthetic RNA controls are presented in **Fig. 5a** and **5b**. The y-axis shows the prevalences, which
363 are the ratios of each variant's concentration to total SARS-CoV-2 concentration. The variant
364 showing the highest prevalence became the dominant variant. If none of the two targets (i.e., Alpha
365 and Delta variants) are higher than 0.5, the Others, which indicate all SARS-CoV-2 lineages other
366 than our target variants (i.e., the Alpha and Delta variant), became the dominant variant. With the
367 highest total virus concentrations (10^4 gc/ μ L), our RT-qPCR assays successfully assign the correct
368 dominant variant to all experimental cases ($p < 0.001$) (**Fig. 5a**). For example, in the case of the
369 mixtures between WT and Alpha variant, we assigned Alpha variant to the RNA mixtures whose
370 actual prevalence of Alpha variant were 0.7 and 0.9 whereas we assigned 'Others' when the
371 prevalence of Alpha variant were 0.1 and 0.3. In the same manner, we also assigned the dominant
372 variant correctly to the mixtures of Alpha and Delta variants. Specifically, we assigned the Alpha
373 variant when the actual prevalences of Alpha variant were 0.7 and 0.9. At the same time, the Delta
374 variant was assigned to the other two mixtures whose prevalences of Alpha variant were 0.1 and
375 0.3. In addition, we found that the PCR assays assigned the dominant variant correctly when the
376 total virus concentrations were 10^1 gc/ μ L for all mixing ratios (**Fig. 5b**). However, the statistical
377 analysis showed that the comparisons of prevalences determined by the RT-qPCR were significant
378 only when the mixing ratios were 0.9:0.1 or vice versa for mixtures of WT and Alpha variant or
379 Alpha variant and Delta variant. Note that when total virus concentrations were 10^1 gc/ μ L,
380 concentrations of each synthetic RNA control were ranging from 1×10^0 to 9×10^0 gc/ μ L depending

381 on the mixing ratios, which were less than their LOQs (10^1 gc/ μ L). Based on these findings, we
382 concluded that our RT-qPCR assays could find the dominant variant when total SARS-CoV-2
383 concentrations are higher than LOQs (10^1 gc/ μ L) and the prevalence of target variants is higher
384 than 0.9 (**Fig. 5b**). When the total SARS-CoV-2 concentrations become higher, Alpha and Delta
385 variant concentrations are higher than LOQs of the RT-qPCR assays (10^1 gc/ μ L), our RT-qPCR
386 assays can assign the dominant variant when its prevalence is higher than 0.7 (**Fig. 5a**).

387

388



389

390 **Fig. 5.** The dominant variants of the mixtures of synthetic RNA controls determined by RT-qPCR
 391 assays. Total SARS-CoV-2 concentrations were determined by the N gene concentrations at (a)
 392 10⁴ gc/μL and (b) 10¹ gc/μL. Prevalences on the y-axis indicate the ratio of each variant'
 393 concentration to the total virus concentrations. The x-axis presented the mixing ratios of different
 394 synthetic RNA controls (W, A, and D stand for WT, Alpha variant and Delta variant, respectively).
 395 Decisions made on top of each graph showed the dominant variant determined by the RT-qPCR
 396 assays. One sample t-test or two-sample t-test were conducted to compare prevalence between
 397 Alpha variant and 0.5 or the prevalences between Alpha and Delta variants (ns: p>0.05, *:
 398 0.001<p<0.05, **:p<0.001), respectively.

399

400 Application of PCR assays to sewage samples and confirmation by NGS

401 We applied our PCR assays to six different local sewage samples. We first obtained RNA
 402 extracts from those sewage samples. The total SARS-CoV-2 concentrations (i.e., N gene) of these
 403 RNA extracts ranged from 1.4 × 10¹ to 1.8 × 10² gc/μL (SI Table 3). After accounting for

404 recovery efficiencies and concentration factors, the SARS-CoV-2 concentrations (i.e., N gene) of
405 these sewage samples ranged from 1.3×10^3 to 6.0×10^4 gc/L (**Eq. 3**). These concentrations
406 agree with the SARS-CoV-2 concentrations of sewage samples analyzed previously (24). Then,
407 we determined the prevalence of variants based on the ratios of the Alpha variant concentration
408 (determined by PRIMES-designed PCR) over the total SARS-CoV-2 (N gene). We found that
409 sample #1 has 0.85 prevalence of the Alpha variant. Based on the results with the RNA synthetic
410 mixtures, we assigned the Alpha variant as a dominant variant to sample #1. Similarly, we
411 assigned the Delta variant to Sample #5 and #6 because of their prevalences of 0.92 and 0.73,
412 respectively. On the other hand, none of the Alpha and Delta variants presented higher than 0.5
413 prevalence for Sample #2, #3, and #4, so we assigned Others to these three samples.

414 To further confirm whether the RT-qPCR results were correct, we conducted NGS analysis
415 to examine eight mutation markers for the Alpha variant (S: Δ 69/70, S: Δ 144, S:N501Y, S:A570D,
416 S:P681H, S:T716I, S:S982A, and S:D1118H) and six mutation markers for the Delta variant
417 (S:T19R, S: Δ 156/157, S:L452R, S:T478K, S:P681R, and S:D950N) on the spike gene of two
418 sewage samples (#5 and 6) and three synthetic RNA controls (WT, Alpha, and Delta variant).
419 Samples #1, #2, #3, and #4 were not appropriate for sequencing due to the low SARS-CoV-2
420 concentrations ($<10^2$ gc/ μ L). From Sample #5 and #6 classified to the Delta variant by the RT-
421 qPCR assays, we detected all six mutations for the Delta variant. In comparison, none of the eight
422 mutations for the Alpha variant were detected in these samples. We believe the NGS analyses were
423 reliable because of the results with the synthetic RNA controls. We detected all mutation markers
424 with corresponding synthetic RNA controls. For example, we detected the eight Alpha variant
425 mutations from the Alpha variant RNA samples and found the six Delta variant mutations from
426 Delta variant RNA controls (**Table 1**). Therefore, the agreement between the NGS analysis and

427 RT-qPCR assays supports that our RT-qPCR can assign the most likely variant for the local sewage
 428 samples.

429

430 **Table 1.** Comparisons between RT-qPCR assays and NGS analysis

Sample	Mutation markers for Alpha variant								Mutation markers for Delta variant					
	$\Delta 69/70$	$\Delta 144$	N501Y	A570D	P681H	T716I	S982A	D1118H	T19R	$\Delta 156/157$	L452R	T478K	P681R	D950N
RNA for WT	Gray	Gray	Gray	Gray	Gray	Gray	Gray	Gray	Gray	Gray	Gray	Gray	Gray	Gray
RNA for Alpha variant	Orange	Orange	Orange	Orange	Orange	Orange	Orange	Orange	Gray	Gray	Gray	Gray	Gray	Gray
RNA for Delta variant	Gray	Gray	Gray	Gray	Gray	Gray	Gray	Gray	Orange	Orange	Orange	Orange	Orange	Orange
Sewage #5	Gray	Gray	Gray	Gray	Gray	Gray	Gray	Gray	Orange	Orange	Orange	Orange	Orange	Orange
Sewage #6	Gray	Gray	Gray	Gray	Gray	Gray	Gray	Gray	Orange	Orange	Orange	Orange	Orange	Orange

431 1) Orange color represents that mutations are detected while gray color indicates that
 432 mutations are not detected.

433

434 Discussion

435 PCR assays have advantages for SARS-CoV-2 variant detection in sewage over sequencing
 436 technologies such as low cost, fast turnaround, and robustness to environmental samples. However,
 437 PCR assays can examine only a few mutations due to size constraints of primer and probe
 438 sequences, compromising their accuracy as distinct SARS-CoV-2 lineages may share target
 439 mutations. We used the PRIMES algorithm to show that the current variant-specific PCR assays
 440 have diminished accuracy when applied outside the region where they were developed. These
 441 findings suggest that considering regional and temporal dynamics of variants is important to secure
 442 the sensitivity and specificity of PCR assays that target only a limited number of mutations.
 443 Subsequently, we used PRIMES and open-source databases (e.g., GISAID, Pangolin, or

444 outbreak.info) to design PCR primers to determine the dominant SARS-CoV-2 variants (i.e.,
445 Alpha and Delta variant) in local sewage samples.

446 The regional and temporal variations are especially critical for SARS-CoV-2 detection
447 because various SARS-CoV-2 lineages with different genotypes have been reported across the
448 world. Commercial PCR kits for variant detection are currently available. However, these kits also
449 target a few mutation markers originating from SARS-CoV-2 lineages of interest (25–27). As we
450 showed above, targeting a single mutation could make the assay less accurate at certain regions
451 due to the presence of other lineages that have the same mutation. In addition, our findings are not
452 limited to PCR assays, but are also relevant for the other types of molecular assays such as loop-
453 mediated isothermal amplification (LAMP), PfuAgo-based assay, and Clustered, Regularly-
454 Interspaced Short Palindromic Repeats (CRISPR)-based assays that are designed to detect specific
455 RNA sequences for virus detection (28–30). For example, two LAMP assays that target N genes
456 for SARS-CoV-2 test could have low accuracy when applied outside of Germany or the US, where
457 the assays were developed and verified with clinical samples (28, 31). This low accuracy issue
458 could happen because their primers include sequences for [N:A119S](#), a mutation marker for the
459 Zeta variant (P.2 lineage). The Zeta variant was dominant in some South American countries
460 (Suriname, Paraguay, Uruguay, and Brazil). [Zhang et al.](#) (2021) (32) designed a LAMP assay
461 targeting the ORF1a gene, but their F2 primer includes sequences for ORF1a:V86F and F1 primer
462 ORF1:E102K. The Food and Drug Administration (FDA) also recommended that mutations
463 present in the sequences where molecular diagnostic tests target for virus detection should be
464 monitored by *in silico* analysis (33). Our PRIMES tool allows users and developers of molecular
465 diagnostic assays to follow this recommendation.

466 Perfect loci to target viral mutation are not realistic because viruses evolve randomly, so
467 one that looks perfect could be affected by emerging variants. For example, the S:Δ69/70 mutation
468 used to be a unique mutation for the Alpha variant, but the Eta variant, which appeared later, also
469 has the same mutation. Thus, if the S:Δ69/70 is considered an exclusive mutation to the Alpha
470 variant, the Eta variant will be false positive for the Alpha variant. In addition, sub-lineages in the
471 target variant may not have one of the mutation markers for the target variant. For example, less
472 than 0.5% of Q.4 (one of the sub-lineages for the Alpha variant and reported December 2020) is
473 known to have a S:P681H. The S:P681H mutation is one of the mutation markers for the Alpha
474 variant. Thus, if S:P681H mutation is targeted for the Alpha variant, Q.4 will cause false negatives.
475 These examples demonstrate that PCR assays could have different sensitivities and specificities
476 depending on various lineages of SARS-CoV-2 that coexist with the target lineage.

477 Global genomic databases for emergent variants have greatly improved since the onset of
478 COVID-19 pandemics (34). Before COVID-19, influenza sequences are archived in GISAID. Fast
479 mutating pathogens such as influenza and coronavirus should be monitored because they have
480 pandemic potential. As we showed in this study, assays targeting these pathogens need to keep up
481 with their evolution, and the developed methodology facilitates genomic surveillance of any fast
482 mutating pathogen.

483

484 **Methods**

485 **Sewage samples**

486 We followed the Minimum information Environmental Microbiology Minimum Information
487 (MIQE) Guidelines to ensure the credibility and reproducibility of our data (35). Detailed
488 information on the MIQE is summarized in **SI Table 4**. Also, detailed information from sample

489 collection to data analysis is described in **SI Table 5**. Briefly, we used ISCO automatic samplers
490 (6712 ISCO, Teledyne ISCO, USA) to collect three-day composite sewages (about 2 L) from the
491 sewer distribution system across Champaign County, IL, USA. $MgCl_2$ was added to the sewage
492 samples at the final concentration of 50 mM to facilitate the coagulation of viruses and sewage
493 sludge. We kept sewage samples on ice while moving them to our laboratory in 2 hours. We gently
494 removed the supernatant upon arrival and added 200 μ L of bovine coronavirus (BCoV) to the
495 remaining solution (about 50 mL) to determine virus recovery efficiency. After 5 minutes of
496 incubation at room temperature, we centrifuged the mixture at 10,000 rpm (13,900 g) for 30
497 minutes (Sorvall Legend RT Plus, Thermo Fisher Scientific, USA). The supernatant was discarded
498 again, and the sludge (about 1 g) was taken to harvest viruses. Then, we extracted viral RNA from
499 the sludge using the Viral RNA extraction Mini Kit (Qiagen, Germany) following the
500 manufacturer's procedure. The RNA extracts were purified using an RNA purification kit (RNeasy
501 MinElute Cleanup Kit, Qiagen, German) to reduce the PCR inhibitions. It took less than 9 hours
502 from sample collection to RNA extraction. The RNA samples were stored at -80°C until
503 downstream analyses were ready. The same sample preparation processes were applied to
504 drainages discharged from a food processing industry whenever we processed sewage samples.
505 There are no sources of human feces that merged to these drainages, which were therefore used
506 for negative controls. Indeed, we did not detect any SARS-CoV-2 from these negative controls.
507 Therefore, we are confident there were no false positives for SARS-CoV-2 in our sewage samples.
508 With the concentrations of RNA extracts, we used Eqs. 3-5 to determine the virus concentrations
509 in sewage samples.

510

$$511 \quad C_{Sewage} (gc/L) = C_{RNA\ extract} (gc/\mu L) \times \frac{Concentration\ factor\ (\mu L/L)}{Recovery\ efficiency} \quad (Eq. 3)$$

512 $Concentration\ factor\ (\mu L/L) = \frac{Volume\ of\ RNA\ extract\ (\mu L)}{Volume\ of\ initial\ sewage\ (L)}$ (Eq. 4)

513 $Recovery\ efficiency = \frac{The\ number\ of\ BCoV\ in\ RNA\ extract}{The\ number\ of\ BCoV\ in\ initial\ sewage}$ (Eq. 5)

514

515 **Determination of LODs and LOQs**

516 We first determined the limit of detection (LOD) and the limit of quantification (LOQ) for
517 Alpha and Delta variants with serial dilutions of the synthetic RNA controls. We prepared 10-fold
518 serial dilutions of synthetic RNA controls and determined a positive sample fraction at each
519 concentration. The number of replicates for concentrations near LOD are 20 while the sample
520 numbers for the higher concentration were 4. We used a sigmoidal function (Eq. 6) to determine
521 the trend lines for fraction positive samples with different concentrations and calculated the LODs
522 (36).

523

524 $Y = \frac{I}{1 + e^{-a - b \times \log(X)}}$ (Eq. 6)

525

526 where X is gene copy (gc/ μ L), Y means positive rate, and both a and b are constants. LOQ was
527 defined as the lowest concentration with coefficient of variation (CV) less than 35% (36). We
528 calculated CV by Eq. 7.

529

530 $CV = \sqrt{(1 + E)^{(SD)^2 \times \ln(1 + E)} - 1}$ (Eq. 7)

531

532 where E is a qPCR efficiency, SD is a standard deviation of Cq values.

533

534 **PCR assays for SARS-CoV-2 variant detection in synthetic RNA control**

535 We applied the RT-qPCR assays to 10-fold serial dilutions of synthetic RNA controls to determine
536 LOQs and LODs. LOQ was defined as the lowest concentration with coefficient of variation (CV)
537 less than 35% (36) and LOD was defined as the concentration at which RNA samples test positive
538 (i.e., $C_q < 40$) with 95% probability. For example, we applied the RT-qPCR assay for Alpha variant
539 to 10-fold serial dilutions of Alpha variant RNA controls and those of the WT RNA controls, then
540 compared the C_q values from Alpha variant and WT.

541 We applied each of RT-qPCR assays for Alpha and Delta variant to the synthetic controls
542 of its target variant and WT to determine the cross-reactivity. This process is important because
543 our assays for the Alpha and Delta variants were designed to detect only a SNP of target variants
544 among other lineages that do not have the same SNP. In this experiment, we mixed synthetic RNA
545 controls of WT and Alpha variant or Alpha and Delta variant because these two mixtures
546 represented the transitions where one dominant variant was replaced by the other one in our
547 community. For instance, the Others (mainly B.1.2) were dominant until February 2021 and the
548 Alpha variant raced for the dominant variant in around March 2021. Also, the Alpha variant was
549 dominant from April and May in 2021, but the Delta variants competed with the Alpha variant in
550 around June 2021 (**Fig. 4b**). Total SARS-CoV-2 concentrations (i.e., N gene concentrations) of
551 the mixtures were 10^4 and 10^1 gc/ μ L, which are the reasonable concentration range of SARS-CoV-
552 2 of local sewage samples (24). Also, we mixed the two different RNA controls with four different
553 ratios (i.e., 9:1, 7:3, 3:7, and 1:9) to mimic different scenarios of variant dynamics.

554

555 **PCR assays for SARS-CoV-2 variant detection in sewage samples**

556 We conducted six different RT-qPCR assays to analyze sewage samples. Three of them targeted
557 different loci of SARS-CoV-2 genome for virus quantification and the dominant variant detection.
558 The other three assays were applied to measure bovine coronavirus (BCoV), pepper mild mottle
559 virus (PMMoV), and Tulane virus (TV), which were used for calculation of virus recovery
560 efficiency, normalization of SARS-CoV-2 to human feces, and inhibition tests, respectively. 2-
561 fold diluted the RNA samples in molecular biology grade water (Milliporesigma, USA) before the
562 quantification. We used Taqman-based RT-qPCR for the N1 gene detection as suggested by CDC
563 and SYBR-based RT-qPCR for the other six assays (**SI Table 6**). The SYBR-based RT-qPCR
564 started with mixing the 3 μL of viral genome with 5 μL of $2 \times$ iTaq universal SYBR green reaction
565 mix, 0.125 μL of iScript reverse transcriptase from the iTaq universal SYBR green reaction mix
566 (Bio-Rad Laboratories, USA), 0.3 μL of 10 μM forward primer for each virus, 0.3 μL of 10 μM
567 reverse primer for each virus, and 1.275 μL of molecular biology grade water (Corning, NY, USA).
568 The PCR cocktail for the one-step RT-qPCR was placed in 96-well plates (4306737, Applied
569 Biosystems, USA) and analyzed by a qPCR system (QuantStudio 3, Thermo Fisher Scientific,
570 USA). The thermocycle began with 10 minutes at 50°C and 1 minute at 90°C followed by 40 cycles
571 of 30 seconds at 60°C and 1 minute at 90°C. The Taqman-based RT-qPCR was initiated by mixing
572 5 μL of viral genome with 5 μL of Taqman Fast Virus 1-step Master Mix (4444432, Applied
573 Biosystems, USA), 1.5 μL of primers/probe mixture for N1 gene (2019-nCoV RUO kit, Integrated
574 DNA Technologies, USA), and 8.5 μL of water. The 20 μL of mixture was analyzed by the same
575 qPCR system as used for the SYBR-based RT-qPCR, except for a different thermal cycle (5
576 minutes at 50°C, 20 seconds at 95°C followed by 45 cycles of 3 seconds at 95°C and 30 seconds
577 at 55°C). We used synthetic RNA controls to get standard curves for WT, Alpha variant, and Delta

578 variant (TWIST Bioscience, USA, Part numbers are 102024, 103907, and 104533, respectively).
579 The PCR standard curves were obtained for every RT-qPCR analysis with 10-fold serial dilutions
580 of synthetic RNA controls and PCR efficiencies for RT-qPCR were higher than 85% ($R^2 > 0.99$).
581 The SYBR signal was normalized to the ROX reference dye. The cycle of quantification (Cq)
582 values was determined automatically by QuantStudio™ Design & Analysis Software (v1.5.1).
583 Based on the melting curves, the primers were specifically bound to the target genome. The
584 numbers of technical replicates were 4 for synthetic RNA controls and 3 for sewage samples except
585 for LODs and LOQs determination where 20 replicates were analyzed.

586

587 **Next-generation sequencing to assign SARS-CoV-2 lineages**

588 The PCR results were confirmed by sequencing the spike gene of three controls (wild type, alpha
589 variant, delta variant) and two sewage samples (#5 and #6) were performed on the Illumina MiSeq
590 platform. A set of four pairs of primers in-house designed were used to amplify the spike of RNA
591 samples using SuperScript™ III One-Step RT-PCR System with Platinum™ Taq High Fidelity
592 DNA Polymerase (ThermoFisher). Amplicons were purified using QIAquick PCR Purification Kit
593 (Qiagen), quantified using Qubit fluorometer, and subject to library preparation using Nextera XT
594 kit and sequencing on MiSeq.

595

596 **Data availability**

597 All the sequence data analyzed in this study is publicly available at GISAID
598 (<https://www.gisaid.org/>). The analyzed and processed real data results are available at
599 <https://github.com/elkebir-group/primes-data>.

600

601 **Code availability**

602 The code has been deposited on Github at <https://github.com/elkebir-group/primes>.

603

604 **Acknowledgement:**

605 We acknowledge the funding from the Grainger College of Engineering and the JUMP-ARCHES
606 program of OSF Healthcare in conjunction with the University of Illinois. Sequencing was funded
607 in part by the Food and Drug Administration Veterinary Laboratory Investigation and Response
608 Network (FOA PAR-17-141) under grant 1U18FD006673-01. M.E-K. acknowledges the National
609 Science Foundation (grants: CCF-2027669 and CCF-2046488). The authors also acknowledge
610 Bill Brown for sampling site selection, Hayden Wennerdahl, Kip Stevenson, Dr. Laura Keefer and
611 Dr. Schmidt for sampling deployment, and Yuqing Mao, Matthew Robert Loula, Aashna Patra,
612 Kristin Joy Anderson, Mikayla Diedrick, Hubert Lyu, Hamza Elmahi Mohamed, Jad R Karajeh,
613 Runsen Ning, Rui Fu, Kate O'Brien, Nathan Kim for sewage sampling and processing.

614

615

616 **Reference**

- 617 1. Harvey WT, Carabelli AM, Jackson B, Gupta RK, Thomson EC, Harrison EM, Ludden C,
618 Reeve R, Rambaut A, Peacock SJ, Robertson DL. 2021. SARS-CoV-2 variants, spike
619 mutations and immune escape. *Nat Rev Microbiol* 2021 19:409–424.
- 620 2. I L, V P, D M, M C. 2021. Immune Evasion of SARS-CoV-2 Emerging Variants: What
621 Have We Learnt So Far? *Viruses* 13.
- 622 3. Grubaugh ND, Hodcroft EB, Fauver JR, Phelan AL, Cevik M. 2021. Public health actions
623 to control new SARS-CoV-2 variants. *Cell* 184:1127–1132.
- 624 4. Peccia J, Zulli A, Brackney DE, Grubaugh ND, Kaplan EH, Casanovas-Massana A, Ko
625 AI, Malik AA, Wang D, Wang M, Warren JL, Weinberger DM, Arnold W, Omer SB.
626 2020. Measurement of SARS-CoV-2 RNA in wastewater tracks community infection
627 dynamics. *Nat Biotechnol* 2020 38:1164–1167.
- 628 5. Larsen DA, Wigginton KR. 2020. Tracking COVID-19 with wastewater. *Nat Biotechnol*
629 2020 38:1151–1153.
- 630 6. Ahmed W, Angel N, Edson J, Bibby K, Bivins A, O’Brien JW, Choi PM, Kitajima M,
631 Simpson SL, Li J, Tschärke B, Verhagen R, Smith WJM, Zaugg J, Dierens L, Hugenholtz
632 P, Thomas K V., Mueller JF. 2020. First confirmed detection of SARS-CoV-2 in untreated
633 wastewater in Australia: A proof of concept for the wastewater surveillance of COVID-19
634 in the community. *Sci Total Environ* 728:138764.
- 635 7. Prado T, Fumian TM, Mannarino CF, Resende PC, Motta FC, Eppinghaus ALF, Chagas
636 do Vale VH, Braz RMS, de Andrade J da SR, Maranhão AG, Miagostovich MP. 2021.
637 Wastewater-based epidemiology as a useful tool to track SARS-CoV-2 and support public
638 health policies at municipal level in Brazil. *Water Res* 191:116810.

- 639 8. Gonzalez R, Curtis K, Bivins A, Bibby K, Weir MH, Yetka K, Thompson H, Keeling D,
640 Mitchell J, Gonzalez D. 2020. COVID-19 surveillance in Southeastern Virginia using
641 wastewater-based epidemiology. *Water Res* 186:116296.
- 642 9. Saththasivam J, El-Malah SS, Gomez TA, Jabbar KA, Remanan R, Krishnankutty AK,
643 Ogunbiyi O, Rasool K, Ashhab S, Rashkeev S, Bensaad M, Ahmed AA, Mohamoud YA,
644 Malek JA, Abu Raddad LJ, Jeremijenko A, Abu Halaweh HA, Lawler J, Mahmoud KA.
645 2021. COVID-19 (SARS-CoV-2) outbreak monitoring using wastewater-based
646 epidemiology in Qatar. *Sci Total Environ* 774:145608.
- 647 10. Hart OE, Halden RU. 2020. Computational analysis of SARS-CoV-2/COVID-19
648 surveillance by wastewater-based epidemiology locally and globally: Feasibility,
649 economy, opportunities and challenges. *Sci Total Environ* 730:138875.
- 650 11. Wang H, Miller JA, Verghese M, Sibai M, Solis D, Mfuh KO, Jiang B, Iwai N, Mar M,
651 Huang C, Yamamoto F, Sahoo MK, Zehnder J, Pinsky BA. 2021. Multiplex SARS-CoV-2
652 Genotyping Reverse Transcriptase PCR for Population-Level Variant Screening and
653 Epidemiologic Surveillance. *J Clin Microbiol* 59.
- 654 12. Guglielmi G. 2020. The explosion of new coronavirus tests that could help to end the
655 pandemic. *Nature* 583:506–509.
- 656 13. Lin Lee W, Imakaev M, Armas F, McElroy KA, Gu X, Duvallet C, Chandra F, Chen H,
657 Leifels M, Mendola S, Floyd-O R, Powell MM, Wilson ST, J Berge KL, J Lim CY, Wu F,
658 Xiao A, Moniz K, Ghaeli N, Matus M, Thompson J, Alm EJ. 2021. Quantitative SARS-
659 CoV-2 Alpha Variant B.1.1.7 Tracking in Wastewater by Allele-Specific RT-qPCR. *Cite*
660 *This Environ Sci Technol Lett* 8:675–682.
- 661 14. CoVariants.

- 662 15. Shu Y, McCauley J. 2017. GISAID: Global initiative on sharing all influenza data – from
663 vision to reality. *Eurosurveillance* 22:30494.
- 664 16. Elbe S, Buckland-Merrett G. 2017. Data, disease and diplomacy: GISAID’s innovative
665 contribution to global health. *Glob Challenges* 1:33–46.
- 666 17. Yaniv K, Ozer E, Shagan M, Lakkakula S, Plotkin N, Bhandarkar NS, Kushmaro A. 2021.
667 Direct RT-qPCR assay for SARS-CoV-2 variants of concern (Alpha, B.1.1.7 and Beta,
668 B.1.351) detection and quantification in wastewater. *Environ Res* 201:111653.
- 669 18. Lin Lee W, Gu X, Armas F, Chandra F, Chen H, Wu F, Leifels M, Xiao A, Jun Desmond
670 Chua F, Kwok GW, Jolly S, Lim CY, Thompson J, Alm EJ, Affiliations A. Quantitative
671 SARS-CoV-2 tracking of variants Delta, Delta plus, Kappa and Beta in wastewater by
672 allele-specific RT-qPCR <https://doi.org/10.1101/2021.08.03.21261298>.
- 673 19. O’Toole Á, Hill V, Pybus OG, Watts A, Bogoch II, Khan K, Messina JP, consortium TC-
674 19 GU (COG-U, (NGS-SA) N for GS in SA, Network B-UCG, Tegally H, Lessells RR,
675 Giandhari J, Pillay S, Tumedi KA, Nyepetsi G, Kebabonye M, Matsheka M, Mine M,
676 Tokajian S, Hassan H, Salloum T, Merhi G, Koweyes J, Geoghegan JL, de Ligt J, Ren X,
677 Storey M, Freed NE, Pattabiraman C, Prasad P, Desai AS, Vasanthapuram R, Schulz TF,
678 Steinbrück L, Stadler T, Consortium SVS, Parisi A, Bianco A, García de Viedma D,
679 Buenestado-Serrano S, Borges V, Isidro J, Duarte S, Gomes JP, Zuckerman NS,
680 Mandelboim M, Mor O, Seemann T, Arnott A, Draper J, Gall M, Rawlinson W, Deveson
681 I, Schlebusch S, McMahon J, Leong L, Lim CK, Chironna M, Loconsole D, Bal A, Josset
682 L, Holmes E, St. George K, Lasek-Nesselquist E, Sikkema RS, Oude Munnink B,
683 Koopmans M, Brytting M, Sudha rani V, Pavani S, Smura T, Heim A, Kurkela S, Umair
684 M, Salman M, Bartolini B, Rueca M, Drosten C, Wolff T, Silander O, Eggink D, Reusken

- 685 C, Vennema H, Park A, Carrington C, Sahadeo N, Carr M, Gonzalez G, Diego SAS,
686 Laboratory NVR, SeqCOVID-Spain, (DCGC) DC-19 GC, (CDGN) CDGN, program
687 DNS-C-2 surveillance, (KDCA) D of EID, de Oliveira T, Faria N, Rambaut A, Kraemer
688 MUG. 2021. Tracking the international spread of SARS-CoV-2 lineages B.1.1.7 and
689 B.1.351/501Y-V2. Wellcome Open Res 2021 6:121.
- 690 20. Li H. 2018. Minimap2: pairwise alignment for nucleotide sequences. *Bioinformatics*
691 34:3094–3100.
- 692 21. Carcereny A, Martínez-Velázquez A, Bosch A, Allende A, Truchado P, Cascales J, Jesús
693 J, Romalde L, Lois M, Polo D, Sánchez G, Pérez-Cataluñ A, Díaz-Reolid A, Antón A,
694 Gregori J, Garcia-Cehic D, Quer J, Palau M, Ruano CG, Pintó RM, Guix S. 2021.
695 Monitoring Emergence of the SARS-CoV-2 B.1.1.7 Variant through the Spanish National
696 SARS-CoV-2 Wastewater Surveillance System (VATar COVID-19). *Cite This Environ*
697 *Sci Technol* 55:11756–11766.
- 698 22. Li Q, Wu J, Nie J, Zhang L, Hao H, Liu S, Zhao C, Zhang Q, Liu H, Nie L, Qin H, Wang
699 M, Lu Q, Li X, Sun Q, Liu J, Zhang L, Li X, Huang W, Wang Y. 2020. The Impact of
700 Mutations in SARS-CoV-2 Spike on Viral Infectivity and Antigenicity. *Cell* 182:1284-
701 1294.e9.
- 702 23. Ståhlberg A, Kubista M. 2014. The workflow of single-cell expression profiling using
703 quantitative real-time PCR. <https://doi.org/10.1586/147371592014901154> 14:323–331.
- 704 24. Pecson BM, Darby E, Haas CN, Amha YM, Bartolo M, Danielson R, Dearborn Y, Di
705 Giovanni G, Ferguson C, Fevig S, Gaddis E, Gray D, Lukasik G, Mull B, Olivas L,
706 Olivieri A, Qu Y, SARS-CoV-2 Interlaboratory Consortium. 2021. Reproducibility and
707 sensitivity of 36 methods to quantify the SARS-CoV-2 genetic signal in raw wastewater:

- 708 findings from an interlaboratory methods evaluation in the U.S. *Environ Sci Water Res*
709 *Technol* <https://doi.org/10.1039/d0ew00946f>.
- 710 25. Caza M, Hogan CA, Jassem A, Prystajecy N, Hadzic A, Wilmer A. 2021. Evaluation of
711 the clinical and analytical performance of the Seegene allplex™ SARS-CoV-2 variants I
712 assay for the detection of variants of concern (VOC) and variants of interests (VOI). *J Clin*
713 *Virol* 144:104996.
- 714 26. Chan CT-M, Leung JS-L, Lee L-K, Lo HW-H, Wong EY-K, Wong DS-H, Ng TT-L, Lao
715 H-Y, Lu KK, Jim SH-C, Yau MC-Y, Lam JY-W, Ho AY-M, Luk KS, Yip K-T, Que T-L,
716 To KK-W, Siu GK-H. 2022. A low-cost TaqMan minor groove binder probe-based one-
717 step RT-qPCR assay for rapid identification of N501Y variants of SARS-CoV-2. *J Virol*
718 *Methods* 299:114333.
- 719 27. Hirotsu Y, Omata M. 2021. Detection of R.1 lineage severe acute respiratory syndrome
720 coronavirus 2 (SARS-CoV-2) with spike protein W152L/E484K/G769V mutations in
721 Japan. *PLOS Pathog* 17:e1009619.
- 722 28. Ganguli A, Mostafa A, Berger J, Aydin M, Sun F, Valera E, Cunningham BT, King WP,
723 Bashir R. 2020. Rapid Isothermal Amplification and Portable Detection System for
724 SARS-CoV-2. *PNAS* 1–9.
- 725 29. Broughton JP, Deng X, Yu G, Fasching CL, Servellita V, Singh J, Miao X, Streithorst JA,
726 Granados A, Sotomayor-Gonzalez A, Zorn K, Gopez A, Hsu E, Gu W, Miller S, Pan C-Y,
727 Guevara H, Wadford DA, Chen JS, Chiu CY. 2020. CRISPR–Cas12-based detection of
728 SARS-CoV-2. *Nat Biotechnol* 2020 38:870–874.
- 729 30. Xun G, Lane ST, Petrov VA, Pepa BE, Zhao H. 2021. A rapid, accurate, scalable, and
730 portable testing system for COVID-19 diagnosis. *Nat Commun* 2021 12:1–9.

- 731 31. Thi VLD, Herbst K, Boerner K, Meurer M, Kremer LP, Kirrmaier D, Freistaedter A,
732 Papagiannidis D, Galmozzi C, Stanifer ML, Boulant S, Klein S, Chlanda P, Khalid D,
733 Miranda IB, Schnitzler P, Kräusslich H-G, Knop M, Anders S. 2020. A colorimetric RT-
734 LAMP assay and LAMP-sequencing for detecting SARS-CoV-2 RNA in clinical samples.
735 *Sci Transl Med* 12.
- 736 32. Zhang Y, Odiwuor N, Xiong J, Sun L, Nyaruaba RO, Wei H, Tanner NA, Tanner N.
737 Rapid Molecular Detection of SARS-CoV-2 (COVID-19) Virus RNA Using Colorimetric
738 LAMP <https://doi.org/10.1101/2020.02.26.20028373>.
- 739 33. Genetic Variants of SARS-CoV-2 May Lead to False Negative Results with Molecular
740 Tests for Detection of SARS-CoV-2 - Letter to Clinical Laboratory Staff and Health Care
741 Providers | FDA.
- 742 34. Maier W, Bray S, van den Beek M, Bouvier D, Coraor N, Miladi M, Singh B, De Argila
743 JR, Baker D, Roach N, Gladman S, Coppens F, Martin DP, Lonie A, Grüning B,
744 Kosakovsky Pond SL, Nekrutenko A. 2021. Ready-to-use public infrastructure for global
745 SARS-CoV-2 monitoring. *Nat Biotechnol* 2021 39:1178–1179.
- 746 35. Bustin SA, Benes V, Garson JA, Hellemans J, Huggett J, Kubista M, Mueller R, Nolan T,
747 Pfaffl MW, Shipley GL, Vandesompele J, Wittwer CT. 2009. The MIQE guidelines:
748 Minimum information for publication of quantitative real-time PCR experiments. *Clin*
749 *Chem* 55:611–622.
- 750 36. Forootan A, Sjöback R, Björkman J, Sjögreen B, Linz L, Kubista M. 2017. Methods to
751 determine limit of detection and limit of quantification in quantitative real-time PCR
752 (qPCR). *Biomol Detect Quantif* 12:1–6.
- 753